Performance Prediction for Subsea Structures during Lowering Operations

By

Wei Zhang

National Centre for Maritime Engineering and Hydrodynamics

Australian Maritime College

Academic Supervisors

A/Prof. Shuhong Chai

Dr. Hung Nguyen

Submitted in fulfilment of the requirement for the Master of Philosophy (Maritime Engineering).
University of Tasmania <Jan 2018>

[Page intentionally left blank]

Abstract

Accurate predictions of the hydrodynamic loads experienced by offshore structures with large horizontal surface are crucial for offshore installation operations, especially when the structures are crossing the splash zone. The structures may encounter various wave conditions and experience significant impact forces which lead to unexpected impulsive loads on the hoisting system, and subsequently, the operation window may be limited by the impulsive loads.

The numerical simulations of the water entry process for different objects, such as a cylinder and a wedge, have undergone substantial development in recent years. However, there have not been studies conducted on perforated plates in terms of quantifying the slamming coefficients for various layout configurations. The main objective of this work is to find a viable solution to predict the impact force acting on subsea structures, to improve the safety of offshore lowering operations, especially during the water entry process. To achieve the research objective, the Unsteady Reynolds-averaged Navier-Stokes equations (URANS) solver STAR-CCM+ has been used to predict the slamming coefficients for perforated plates of various perforation ratios and layout configurations (i.e. phase one). OrcaFlex was then used to model the splash zone crossing under different sea states, using the slamming coefficients obtained via STAR-CCM+ and DNV-RP-H103 (i.e. phase two).

In phase one, the URANS solver was verified and validated by predicting the slamming coefficient of a circular cylinder during the water entry process. A good agreement has been achieved between the numerical and experimental results. Upon validating the numerical model, the water entry of perforated plates has been simulated to predict the slamming coefficient and free surface profile at full-scale, where the influence of different layout configurations was investigated. In addition, the effect of air compressibility was found to be important when studying the water entry of the flat plate.

In the second phase, the impact of the slamming coefficient on splash zone crossing has been studied, through a series of time domain simulations for the perforated plate under different sea states using OrcaFlex. The results obtained using the slamming coefficient predicted via STAR-CCM+ and the slamming coefficient recommended in DNV-RP-H103 were compared. The results suggest that the probability of slack occurring is lower when using the recommended slamming coefficient from DNV-RP-H103 for offshore structures

with a large horizontal surface, such as the perforated plate in this study. In addition, the influence of a passive heave compensator (PHC) has been investigated through a series of deployment simulations for the perforated plate with and without a PHC. Based on the results, the presence of the PHC is crucial for installation operations where the wave period ranges from 3 to 10 seconds in order to achieve a safe operation.

In summary, the presented work has provided some insights into the slamming coefficients predicted for perforated plates with various layout configurations. The probability distribution of slack occurring on the hoisting system can assist the field engineer to perform the risk assessment for lowering operations.

Statements and Declarations

Declaration of Originality

This thesis contains no material which has been accepted for a degree or diploma by the University or any other institution, except by way of background information and duly acknowledged in the thesis, and to the best of my knowledge and belief no material previously published or written by another person except where due acknowledgement is made in the text of the thesis, nor does the thesis contain any material that infringes copyright.

Authority of Access

This thesis may be made available for loan and limited copying and communication in accordance with the Copyright Act 1968.

Signed:

Wei Zhang

Date: 26/01/2018

Statement Regarding Published Work Contained in Thesis

The publishers of the papers comprising Chapters three to five hold the copyright for that content, and access to the material should be sought from the respective journals or conference paper. The remaining non-published content of the thesis may be made available for loan and limited copying and communication in accordance with the Copyright Act 1968.

Statement of Co-Authorship

The following people and institutions contributed to the publication of work undertaken as part of this thesis:

- Wei Zhang, University of Tasmania (Candidate)
- A/Prof. Shuhong Chai, University of Tasmania (Co-Author 1)
- Dr. Hung Nguyen, University of Tasmania (Co-Author 2)
- Mr Yuting Jin, University of Tasmania (Co-Author 3)

Publication list and proportion of work details:

Chapter 3-4 (Paper 1) **URANS predictions of the slamming coefficients for the perforated plates during water entry** Paper was accepted by Part A – International Journal of Maritime Engineering [Candidate: 80%, Author 1: 10%, Author 2: 5%, Author 3: 5%]
Chapter 5 (Paper 2) **Lowering Perforated Plate through Splash Zone under Different Sea States** Paper was presented at the 6th Society for Underwater Technology Technical Conference [Candidate: 80%, Author 1: 10%, Author 2: 5%, Author 3: 5%]

We the undersigned agree with the above stated "proportion of work undertaken" for each of the above published (or submitted) peer-reviewed manuscripts contributing to this thesis.

Signed:

Associate Professor Shuhong Chai
Primary Supervisor
National Centre for Maritime Engineering and Hydrodynamics
University of Tasmania

Doctor Hung Nguyen
Co-Supervisor
National Centre for Maritime Engineering and Hydrodynamics
University of Tasmania

Yuting Jin
Co-Author
National Centre for Maritime Engineering and Hydrodynamics
University of Tasmania

26/01/2018

Acknowledgments

This thesis has been carried out for the Master of Philosophy (Maritime Engineering), under the supervision of A/ Prof Shuhong Chai and Dr Hung Nguyen. The work is performed at the Australian Maritime College, University of Tasmania.

I would like to thank my primary supervisor A/ Prof Shuhong Chai for inspiring me and sharing her knowledge with me about this research topic. I would also like to thank Dr Hung Nguyen for his constant support for my research. I also want to express my thanks to my fellows Yuting Jin and Jun Yi Lee for their proofreading. I also like to acknowledge Duncan Roy and Alistair Arnott from Orcina Ltd. for their kind advice about the modelling of environmental loading during lowering operations.

Next, I would like to thank my parents for their constant support during my postgraduate study period. Their encouragement and love motivate me pursuing my study further.

Last, I would like to thank the University of Tasmania for providing the access to Australian Maritime College cluster13 and High-performance computing (HPC) system TPAC.

Table of Contents

List of Figures

List of Tables

Abbreviations

Symbol	Description
URANS	Unsteady Reynolds-averaged Navier-Stokes
CFD	Computational Fluid Dynamics
DAF	Dynamic Amplification Factor
FVM	Finite Volume Method
PHC	Passive Heave Compensator
SST	Shear-Stress Transport
VOF	Volume of Fluid
VIV	Vortex-induced Vibrations
RAO	Response Amplitude Operator

Nomenclature

Roman symbols:

Symbol	Description	Unit
A_p	The project area of object normal to the direction of oscillation	m^2
C_s	Slamming coefficient	-
C_k	Correction factor	-
D/S_c	Benchmark value	-
E	Comparison error	-
F	Fetch length	m
F_s	Slamming impact force	N
f	frequency	Hz
f_m	Peak frequency	Hz
G_B	Base size	m
g	Acceleration due to gravity	$9.81 m/s^2$
h	Perforated plate height	m
H	Dropping height	m
H_s	Significant wave height	m
L	Flow characteristic length scale	m

n	Unit vector in water surface outward normal direction	-
n_s	The number of the slack condition	-
N	The total number of simulation cases	-
p	Pressure	*Pa*
$\bar{p}$	Time-averaged pressure	*Pa*
p_k	Order of accuracy	-
p_{kest}	Limiting order of accuracy	-
P_{slack}	Probability of slack condition	*%*
Q	Volume energy sources	-
r_k	Uniform parameter refinement ratio	-
R	Cylinder radius	*m*
Re	Reynolds number	-
R_k	Convergence ratio	-
S_{ij}	Mean strain rate tensor	-
S_k	Solution result	-
S_{α_i}	Source of sink of the each phase	-
S_1	Finest solution result	-
S_U/S_L	Maximum and minimum oscillation numerical results	-
T	Temperature	℃
t	Time	*s*
T_Z	Zero crossing period	*s*
$\bar{u}_i$	Time-averaged velocity	*m/s*
U_D	Experimental data uncertainty	-
$U_I / U_{GC} / U_T$	Parameter uncertainty (iteration, grid size and time-step size)	-
U_{SN}	Total Numerical uncertainty	-
U_V	Validation uncertainty	-
U_{reqd}	Programmatic validation requirement	-
U_{10}	Wind speed at a height of 10m above the free surface	*m/s*
V_T	Total volume	m^3
V_S	Impact velocity	*m/s*
y_1	The distance between wall and first mesh node	*m*
$y+$	Y plus value	-

Greek symbols:

Symbol	Description	Unit
ρ	Density of seawater	kg/m^3
α	Spectral energy parameter	-
α_i	Volume fraction	-
γ	Peak enhancement factor	-
σ	Spectral width parameters	-
ε_k	Solution change	-
δ	Total prism layer thickness	m
$\delta_{k1}^* / \delta_{SN}$	Numerical error	-
$\delta_{RE_{k1}}^*$	One-term estimates for error	-
δ_D	Data error	-
δ_{SM}	Modelling error	-
μ	Turbulent viscosity	$Kg/m^{-1}s^{-1}$
v	Kinematic viscosity	m^2/s
Δt	Time-step	s
Δt_M	Time increment for moving averaging	s
Δx	Smallest grid size	m
x	Distance downstream from the start of the boundary layer	m
$\mathbf{u}$	Velocity field in Cartesian coordinates	-
∇	$(\partial / \partial x, \partial / \partial y, \partial / \partial z)$	-
e	Specific sensible energy	J
λ	Transport coefficient	-

Chapter 1-4 have been removed for copyright or proprietary reasons.

Content contained in them is incorporated in an article published as: Zhang, W., Chai, S., Nguyen, H., Jin, Y., 2018. URANS prediction of the slamming coefficients for perforated plates during water entry, Royal Institution of Naval Architects. Transactions. Part A. International Journal of Maritime Engineering, 160, (Part A1), 41-55

Chapter 5 has been removed for copyright or proprietary reasons.

It has been published as: Zhang, W., Chai, S., Nguyen, H. D., Jin, Y., 2017. Lowering Perforated Plate through Splash Zone under Different Sea States, Proceedings of the 6th Society for Underwater Technology Technical Conference (SUTTC) 2017, 23-24 November 2017, Haikou, China, 1-7.

6 Conclusions

In this study, two different numerical simulation programs have been used for the performance prediction of perforated plates for splash zone crossing modelling. The first program is the URANS solver STAR-CCM+, which has been employed for calculating the slamming coefficient of the perforated plates. The second program is a non-linear time domain finite element solver OrcaFlex, which is employed to simulate the splash zone crossing of the perforated plate coupled with ship motion and a hoisting system.

To demonstrate the feasibility and accuracy of STAR-CCM+, the water entry of a circular cylinder is simulated. The numerical results have a good agreement with the experimental results. It has been found that the background domain should be large enough to avoid flow reflection. Volumetric control should be applied to the free surface and bottom of objects to refine the mesh to better model the sharp interface between air and liquid. It has been shown that the laminar flow model is the appropriate flow model to predict the slamming event after comparing with other turbulent flow models. Also, it is necessary to achieve a Courant number of 1 or less in the refined mesh region.

Based on the findings from the verification and validation studies, the water entry of perforated plates with various configurations has been investigated. For perforated plates with different ratios, the evacuation of trapped air between the bottom of the plate and free surface through gaps is found to be similar for each perforated plate when the gaps have a small length/width ratio (i.e. smaller than 1.625). For perforated plates with different layout configurations, it is found that the slamming coefficient increased with the increase in length/width ratio until it reaches 19.5. However, a further increase in length/width ratio may impose a negative impact on the escape of air due to the increase in gap number.

It is also found that the compressibility of air should be considered for modelling the water entry of structures with a flat horizontal surface (e.g. perforated plate). The air cushion significantly reduces the slamming force and extends the impact time when the structures are passing through the free surface. However, the influence of air compressibility can be neglected for structures such as a cylinder or a wedge. Through a series of numerical simulations performed for a cylinder and perforated plates using STAR-CCM+, it has been shown that the URANS method is feasible to model the water entry of large and complex offshore structures.

Applying the slamming coefficients predicted using the URANS approach, time domain simulations of splash zone crossing has been carried out using OrcaFlex. The characteristics of a hoisting system and ship motions are taken into account. A case study for the perforated plate has been performed under different wave conditions. In addition, the influence of having a PHC has been investigated through a series of deployment simulations, involving a perforated plate with and without PHC.

When the slamming coefficient predicted using STAR-CCM+ was used, the probability of slack occurring on the hoisting system is higher as compared to the probability obtained using the slamming coefficient recommended by DNV-RP-H103 for offshore structures with a large horizontal surface such as the perforated plate. It is also found that the PHC is useful in terms of reducing the motion of lowered structures and the dynamic impact force during the splash zone crossing. It should be used when the wave period is within the range of 3 to 10 seconds in order to achieve higher operational safety. Based on the modelling of the splash zone crossing, it is implied that the selection of hydrodynamic coefficients and characteristics of the hoisting system should be carefully studied. The coefficients determined from experiments or CFD results are strongly recommended for simulation modelling.

7 Further Work

The numerical research for slamming coefficients of perforated plates has proven the advantages of STAR-CCM+ to simulate the water entry process. It has been found that available experiment results of complex structures are very limited for validation purpose, especially for offshore and subsea structures. Therefore, the need for new experiments to be conducted for further work, structures including perforated plate or more complex structures are suggested.

In the current study, only constant drop velocity test has been investigated, while the free drop condition is another important research aspect. Due to the limited computational resources and time constraints during my study period, the free drop CFD simulation could not be performed for perforated plates to gain a better understanding of water entry process. The slamming coefficients prediction for other types of offshore structures with more complex geometries and configurations are suggested to be conducted if more computational resources can be provided.

Regarding the splash zone modelling, all the results of lowering operation performance are based on using the default RAO values of a typical tank vessel provided by OrcaFlex. Therefore, further comparison study is suggested to carry out if the hydrodynamic responses of different offshore installation vessels are available.

Besides this, the possibility of performing seabed landing using OrcaFlex is also recommended, as the buoyancy force and drag force will play as dominant forces rather than slamming force later in the entire installation process. Also, the crane wire can be the study of interest during this period, as the natural period of the hoisting system increases with the increase of crane wire length. A resonance may occur at a certain water depth which may result in large oscillation of hoisting system and may increase the risk of lowering operation. Therefore, the stability of the structure is the main concern for lowering the structure to the seabed. When the structures are landing on the seabed, there can be the other slamming shock on structures which may also lead to the hoisting line slack. This is out of the scope of work for this current study. This further study will be suggested to be investigated to complete the whole process of offshore lowering operation for future work.

References

Anderson Jr, J. D. 2010. *Fundamentals of aerodynamics*, Tata McGraw-Hill Education.

Campbell, I. & Weynberg, P. 1980. Measurement of parameters affecting slamming.

Cd-Adapco 2014. User guide StarCCM+ version 9.02.

Chuang, S.-L. 1966. Experiments on flat-bottom slamming. *Journal of Ship Research,* 10**,** 10-17.

Chuang, S.-L. 1970. Investigation of impact of rigid and elastic bodies with water. DTIC Document.

Cranemaster 2016. Installation of PLEM modules in the South China Sea. *In:* SUBSEA, P. M. I. P. H. C. O. (ed.). Norway: Ernst-B. Johansen AS

Dnv 2010. Recommended Practice DNV_RP-C205. *Environmental condition and environmental loads.*

Dnv 2011. Recommended Practice DNV_RP-H103. *Modelling and analysis of marine operations.*

Fairlie-Clarke, A. & Tveitnes, T. 2008. Momentum and gravity effects during the constant velocity water entry of wedge-shaped sections. *Ocean Engineering,* 35**,** 706-716.

Faltinsen, O. M. 1990. *Sea loads on ships and offshore structures,* UK, Cambridge University Press.

Gordon, R. B., Grytøyr, G. & Dhaigude, M. Modeling Suction Pile Lowering Through the Splash Zone. *ASME 2013 32nd International Conference on Ocean, Offshore and Arctic Engineering*, 2013. American Society of Mechanical Engineers, V001T01A010-V001T01A010.

Greenhow, M. & Lin, W.-M. 1983. Nonlinear-free surface effects: experiments and theory. DTIC Document.

Hasselmann, K., Barnett, T., Bouws, E., Carlson, H., Cartwright, D., Enke, K., Ewing, J., Gienapp, H., Hasselmann, D. & Kruseman, P. 1973. Measurements of wind-wave growth and swell decay during the Joint North Sea Wave Project (JONSWAP). Deutches Hydrographisches Institut.

Huera-Huarte, F., Jeon, D. & Gharib, M. 2011. Experimental investigation of water slamming loads on panels. *Ocean Engineering,* 38**,** 1347-1355.

Ittc 2008. Uncertainty Analysis in CFD Verification and Validation Methodology and Procedures. *25th International Towing Tank Conference-Recommended Procedures and Guidelines.*

Iwanowski, B., Fujikubo, M. & Yao, T. 1993. Analysis of horizontal water impact of a rigid body with the air cushion effect. *日本造船学会論文集,* 1993**,** 293-302.

Jasak, H. 1996. Error analysis and estimation for finite volume method with applications to fluid flow.

Keprate, A. 2015. Impact of passive heave compensator on offshore lifting. *Journal of Shipping and Ocean Engineering,* 5**,** 14.

Korobkin, A. 1996. Acoustic approximation in the slamming problem. *Journal of Fluid Mechanics,* 318**,** 165-188.

Lasrsen, E. 2013. *Impact loads on circular cylinders.* Master Norwegian university of science and technology.

Leap. 2012. *Tips & Tricks: Turbulence part 2-Wall function and Y+ requirement* [Online]. LEAP Australia. Available: http://www.computationalfluiddynamics.com.au/tips-tricks-turbulence-wall-functions-and-y-requirements/.

Mathworks. 2016. *Smooth* [Online]. Available: http://au.mathworks.com/help/curvefit/smooth.html?searchHighlight=smooth.

Næss, T., Havn, J. & Solaas, F. 2014. On the importance of slamming during installation of structures with large suction anchors. *Ocean Engineering,* 89**,** 13.

Nam, B., Hong, S., Kim, Y. & Kim, J. Analysis of Heave Compensator Effects on Deepwater Lifting Operation. *The Tenth ISOPE Pacific/Asia Offshore Mechanics Symposium*, 2012. International Society of Offshore and Polar Engineers.

Nam, B. W., Hong, S. Y., Kim, Y. S. & Kim, J. W. 2013. Effects of passive and active heave compensators on deepwater lifting operation. *International Journal of Offshore and Polar Engineering,* 23.

Orcina 2016. OrcaFlex Manual. Cumbria, UK: Orcina Ltd.

Orcina Ltd. 2017. F02 Passive Compensation. *OrcaFlex Examples - F Payload Handling.*

Sarkar, A. & Gudmestad, O. T. Splash zone lifting analysis of subsea structures. *ASME 2010 29th International Conference on Ocean, Offshore and Arctic Engineering*, 2010. American Society of Mechanical Engineers, 303-312.

Stern, F., Wilson, R. V., Coleman, H. W. & Paterson, E. G. 2001. Comprehensive approach to verification and validation of CFD simulations—part 1: methodology and procedures. *Journal of fluids engineering,* 123**,** 793-802.

Stringer, R., Zang, J. & Hillis, A. 2014. Unsteady RANS computations of flow around a circular cylinder for a wide range of Reynolds numbers. *Ocean Engineering,* 87**,** 1-9.

Swidan, A., Amin, W., Ranmuthugala, D., Thomas, G. & Penesis, I. 2013. Numerical prediction of symmetric water impact loads on wedge shaped hull form using CFD. *World Journal of Mechanics,* 3**,** 311.

Swidan, A. A., Thomas, G. A., Amin, W., Ranmuthugala, D. & Penesis, I. Numerical investigation of water slamming loads on wave-piercing catamaran hull model. *10th High speed marine vehicles Symposium*, 2014. 1-9.

Tveitnes, T., Fairlie-Clarke, A. & Varyani, K. 2008. An experimental investigation into the constant velocity water entry of wedge-shaped sections. *Ocean Engineering,* 35**,** 1463-1478.

Van Nuffel, D., Vepa, K., De Baere, I., Lava, P., Kersemans, M., Degrieck, J., De Rouck, J. & Van Paepegem, W. 2014. A comparison between the experimental and theoretical impact pressures acting on a horizontal quasi-rigid cylinder during vertical water entry. *Ocean Engineering,* 77**,** 42-54.

Verhagen, J. 1967. The impact of a flat plate on a water surface. *J. Ship Res,* 11**,** 211-223.

Von Karman, T. 1929. The impact on seaplane floats during landing.

Wagner, H. 1932. Über Stoß ‐ und Gleitvorgänge an der Oberfläche von Flüssigkeiten. *ZAMM ‐ Journal of Applied Mathematics and Mechanics/Zeitschrift für Angewandte Mathematik und Mechanik,* 12**,** 193-215.

White, F. M. 2011. *Fluid Mechanics,* McGraw-Hill.

Wilson, R. V., Stern, F., Coleman, H. W. & Paterson, E. G. 2001. Comprehensive approach to verification and validation of CFD simulations—Part 2: Application for RANS simulation of a cargo/container ship. *Journal of Fluids Engineering,* 123**,** 803-810.

Zhang, W., Chai, S., Nguyen, H. & Jin, Y. 2017. URANS predictions of the slamming coefficients for perforated plates during water entry. *Transactions of RINA, Part A: International Journal of Maritime Engineering*.

Zhao, R. & Faltinsen, O. 1993. Water entry of two-dimensional bodies. *Journal of Fluid Mechanics,* 246**,** 593-612.

Zhu, X., Faltinsen, O. M. & Hu, C. 2007. Water entry and exit of a horizontal circular cylinder. *Journal of Offshore Mechanics and Arctic Engineering,* 129**,** 253-264.

Appendix A: Moving Average

The moving average is a method to analyse data by averaging series of points, the smoothing function can be easily applied using MatLab for the post-processing of numerical simulation.

It is a default standard smoothing function, and can be summarized as follows:

$$yy = smooth(y, Span) \tag{A.1}$$

yy is returned vector results after averaging the vector y.

The first few elements of yy are (MathWorks, 2016):

$$\begin{aligned} yy(1) &= y(1) \\ yy(2) &= (y(1) + y(2) + y(3))/3 \\ yy(3) &= (y(1) + y(2) + y(3) + y(4) + y(5))/5 \\ yy(4) &= (y(2) + y(3) + y(4) + y(5) + y(6))/5 \\ &... \end{aligned} \tag{A.2}$$

It is worth mentioning that the span should be an odd number. In this thesis, the span width is selected from 0~0.02 of non-dimensional submergence: VT/R, in order to smooth the plot with confidence.

Appendix B: Validation Assessment

With the aim of validating the numerical results against experimental results, a comparison between the comparison error E and validation uncertainty U_V is shown as following steps:

Step 1: calculate the comparison error:

$$E = D - S = \delta_D - (\delta_{SM} + \delta_{SN}) \tag{B.1}$$

$$E = D - S_c = \delta_D - (\delta_{SM} + \varepsilon_{SN}) \tag{B.2}$$

where D is benchmark data, δ_D is data error, δ_{SM} is modelling error and δ_{SN} is numerical error.

Step 2: calculate the validation uncertainty:

$$U_V^2 = U_D^2 + U_{SN}^2 \tag{B.3}$$

$$U_V^2 = U_D^2 + U_{S_cN}^2 \tag{B.4}$$

where U_D is the data uncertainty and U_{SN} is the numerical uncertainty. The equation (B.2) and (B.4) are corrected solutions. In this section, the validation procedure is presented through interpretation of the validation results.

There will be six combinations if we consider the three variables E , U_V and U_{reqd} :

$$\begin{aligned}
&1.|E| < U_V < U_{reqd} \\
&2.|E| < U_{reqd} < U_V \\
&3.U_{reqd} < |E| < U_V \\
&4.U_V < |E| < U_{reqd} \\
&5.U_V < U_{reqd} < |E| \\
&6.U_{reqd} < U_V < |E|
\end{aligned} \tag{B.5}$$

Please refer to section 5.1 and 5.2 of ITTC (2008), a more detailed discussion is presented for six conditions.

Appendix C: Batch Script Excel Sheet for Pre-Processing

Script Table	Script.txt					
// Example script table. // The script generates separate data files for various wave condition with 50 different wave seeds						
// Case	LoadData	Select Environment WaveHs =	Select Environment WaveTz =	Select Environment WaveTimeOrigin=	Select Environment WaveSeed =	SaveData
1	"basecase.dat"	0.50	3.00	-1500.00	123456	1.dat
2					234567	2.dat
3					345678	3.dat
4					456789	4.dat
5					567900	5.dat
6					679011	6.dat
7					790122	7.dat
8					901233	8.dat
9					1012344	9.dat
10					1123455	10.dat
11					1234566	11.dat
12					1345677	12.dat
13					1456788	13.dat
14					1567899	14.dat
15					1679010	15.dat
16					1790121	16.dat
17					1901232	17.dat
18					2012343	18.dat
19					2123454	19.dat
20					2234565	20.dat
21					2345676	21.dat
22					2456787	22.dat
23					2567898	23.dat
24					2679009	24.dat
25					2790120	25.dat
26					2901231	26.dat
27					3012342	27.dat
28					3123453	28.dat
29					3234564	29.dat
30					3345675	30.dat
31					3456786	31.dat
32					3567897	32.dat
33					3679008	33.dat
34					3790119	34.dat
35					3901230	35.dat
36					4012341	36.dat
37					4123452	37.dat
38					4234563	38.dat
39					4345674	39.dat
40					4456785	40.dat
41					4567896	41.dat
42					4679007	42.dat
43					4790118	43.dat
44					4901229	44.dat
45					5012340	45.dat
46					5123451	46.dat
47					5234562	47.dat
48					5345673	48.dat
49					5456784	49.dat
50					5567895	50.dat
51	"basecase.dat"	0.50	4.00	-1500.00	123456	51.dat
52					234567	52.dat
53					345678	53.dat
54					456789	54.dat
55					567900	55.dat
56					679011	56.dat
57					790122	57.dat

Figure D-1: Batch script excel sheet example for pre-processing

Appendix D: Other Parameters for Inputs to Model Splash Zone Crossing

Operation stages

The splash zone crossing simulation is made up of several stages, each is given a specified duration. To ensure a smooth transient when starting a simulation, a built-up stage is required and numbered stage 0. The duration of this stage should be set to at least one wave period. The detailed stage information is shown as follows:

Table D-1: Simulation stages and durations

Stage no.	Duration (s)	Simulation time at stage end (s)
0	14	0
1	30	30
2	5	35
3	5	40
4	10	50

Crane payout when lowering object through free surface

To lower the perforated plate through the free surface, the length control for winches was applied on the crane wire of hoisting system. The tension control was also applied on the tugger winch to stabilize the perforated plate during the splash zone crossing. In addition, the winches were all set by the individual stage, which means that the different control modes can be switched between different stages during the simulation. The winch data is listed as follows:

Table D-2: Control modes for crane wire and tugger winch

Stage	Stage duration (s)	Simulation time at stage end (s)	Mode	Value
		Crane wire		
Statics			Specified length	2
0	14	0	Length at Stage End	2
1	30	30	Specified payout rate change	0

2	5	35	Specified payout rate change	0.5
3	5	40	Specified payout rate	0.5
4	10	50	Specified payout rate	0.5
		Tugger winch 1&2		
Statics			Specified tension	5
0	14	0	Specified tension	5
1	30	30	Specified tension	5
2	5	35	Specified tension	0
3	5	40	Specified payout	0
4	10	50	Specified payout	0

Note: Tensions and tension changes are in kN; lengths and payout are in m; payout rates in m/s; tension rates of change are in kN/s.

Stiffness profile of passive heave compensator

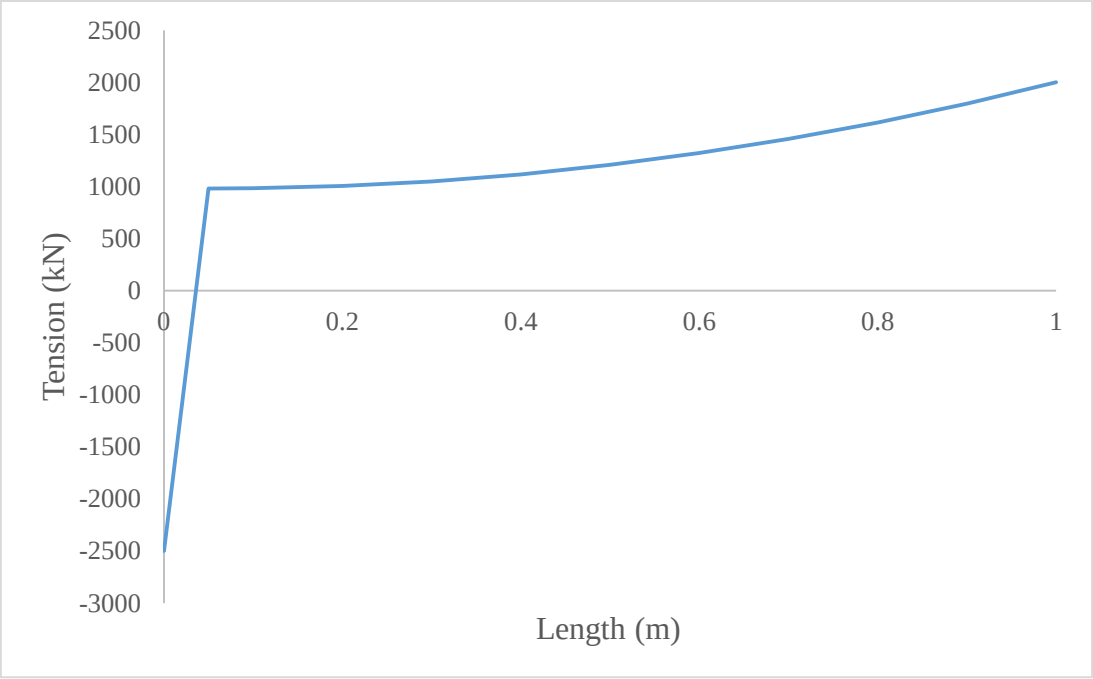

Figure D-2: Stiffness characteristics for passive heave compensator